Importance of Normal Field Continuity in Inhomogeneous Scattering Calculations

Xingchao Yuan, *Member, IEEE*, Daniel R. Lynch, and Keith Paulsen, *Member, IEEE*

Abstract—**The finite element method with conventional scalar bases is coupled with the moment method to handle the three-dimensional scattering and/or absorption from inhomogeneous, arbitrarily shaped objects. The C^0 finite element basis enforces continuity of both normal and tangential E at element boundaries within homogeneous regions. At dielectric interfaces, the continuity of normal D and tangential E are enforced in a strong sense. Excellent agreement between the numerical solution and the Mie series is obtained for both internal and scattered fields for homogeneous and layered spheres under plane wave illumination. Compared to an alternative finite element method using edge elements which lack strong enforcement of normal field continuity, the present method produces higher-order approximations, especially at dielectric interfaces, with no penalties in computational effort.**

I. Introduction

THE hybrid method that combines the method of moments and the finite element method (MoM/FEM) proposed in [1] is a very effective numerical technique for treating electromagnetic scattering from complex inhomogeneous objects. The validity and accuracy of the hybrid formulation for two- and three-dimensional problems are presented in [1] and [2], respectively.

In the FEM portion of [2], we used edge elements which support vector basis functions as proposed in [3]. The development of edge elements has been motivated largely by the need to eliminate parasitic solutions in vector finite element formulations of the Maxwell equations. The success of edge elements in this regard has been discussed and demonstrated in [4], [5]. In our experiences with edge elements [2], [6], it was found that due to the nature of the bases—specifically, the lack of strong enforcement of normal field continuity—high resolution is required near dielectric interfaces. In addition, the computational cost can be as much as twice that required by scalar bases [6].

In previous papers [7], [8], a finite element method using scalar bases has been introduced which provides strong enforcement of both normal $\boldsymbol{D}$ and tangential $\boldsymbol{E}$ continuity across all element boundaries, including those representing dielectric interfaces. Further, the origin of vector parasites in this and other differential-equation-based schemes has been identified in [9], and a simple extension of the FEM weak form implemented on scalar bases rids the calculations of these difficulties [10]. Thus, in terms of eliminating unwanted and spurious solutions in FEM calculations, scalar and vector bases may be considered equivalent. Hence, it becomes important to concentrate on other comparative aspects of the bases, specifically their continuity characteristics for inhomogeneous problems.

In this paper, the FEM weak form recommended in [10] for scalar bases is combined in hybrid fashion with the MoM for solving 3-D scattering problems. The work presented here extends that published in [1], [2], and [10] and has two purposes: 1) to show the validity and accuracy of the method itself, and 2) to provide a direct comparison with solutions that have been generated via edge elements. With regard to the former purpose, numerical solutions are compared with the Mie series for scattering from homogeneous or layered spheres under the illumination of a plane wave. Excellent agreement is obtained for both internal and scattered fields. In terms of the latter objective, the same test cases as those reported in [2] are examined, which allows the effects induced in the computed solutions by the continuity behavior of the respective bases to be compared.

II. Formulation

The detailed formulation of the hybrid moment and finite element method is described in [1]. The basic formulation remains unchanged, irrespective of the choice of bases for the finite element method. To solve 3-D problems, the bases for equivalent sources are chosen the same as those used in [2, Eq. (13)]. Thus, the matrices associated with these bases in [2, Eqs. (4), (5), and (7)] remain formally unchanged.

To use the scalar bases in the finite elements, the electric field $\boldsymbol{E}$ in the interior region is expanded as

$$\boldsymbol{E} = \sum_{j=1}^{N} \boldsymbol{E}_j \phi_j \tag{1}$$

where $\{\boldsymbol{E}_j,\ j = 1,2,\cdots,N\}$ is a set of unknown complex vectors and $\{\phi_j,\ j = 1,2,\cdots,N\}$ is a set of conventional scalar basis functions defined within the volume bounded by a surface S. By definition, ϕ_j are continuous with piecewise continuous first derivatives. The expansion in (1) therefore guarantees appropriate continuity of $\boldsymbol{n}\times\boldsymbol{E}$ and $\boldsymbol{n}\cdot\boldsymbol{D}$ in homogenous or continuously varying media.

At dielectric interfaces where electric properties change abruptly, we follow the strategy given initially in [7]. Conceptually, the FEM grid is severed at an interface separating two electrically distinct regions such that two coincident sets of nodes exist, with separate nodal values $\boldsymbol{E}_{i1}$ and $\boldsymbol{E}_{i2}$ for either side (1,2) of the interface. On assembly of the algebraic system of equations, one of the unknowns $\boldsymbol{E}_i$ is removed in

Manuscript received June 18, 1990; revised November 27, 1990. This paper was supported in part by the National Institutes of Health (Grants RO1 CA37245 and CA45357) and the National Science Foundation (Grant CEE-835-2226).

The authors are with the Thayer School of Engineering, Dartmouth College, Hanover, NH 03755.

IEEE Log Number 9042504.

0018-9480/91/0400-0638$01.00 ©1991 IEEE

favor of the other by enforcing

$$\hat{n}_i \cdot (\epsilon_1^* E_{i1} - \epsilon_2^* E_{i2}) = 0 \tag{2a}$$

$$\hat{n}_i \times (E_{i1} - E_{i2}) = 0 \tag{2b}$$

for each node i. The details of the algebra can be found in [8].

The implementation of this strategy requires definition of a local "nodal normal" $\hat{n}_i$. In common practice, the numerical boundary is a piecewise approximation to the actual physical one, with a discontinuous normal direction at the nodes. The approach adopted here, as well as in our other work [7], [8], [10], [11], is based on the flux and circulation integrals over a material interface

$$\int \hat{n} \cdot (\epsilon_1^* E_1 - \epsilon_2^* E_2)\, ds = 0 \tag{3a}$$

$$\int \hat{n} \times (E_1 - E_2)\, ds = 0. \tag{3b}$$

Substitution of (1) for E results in

$$\sum_{i=1}^{N} (\epsilon_1^* E_{i1} - \epsilon_2^* E_{i2}) \cdot \int \hat{n} \phi_i\, ds = 0 \tag{4a}$$

$$\sum_{i=1}^{N} (E_{i1} - E_{i2}) \times \int \hat{n} \phi_i\, ds = 0 \tag{4b}$$

for which local term-by-term enforcement gives rise to

$$\hat{n}_i = \frac{\int \hat{n} \phi_i\, ds}{\left| \int \hat{n} \phi_i\, ds \right|}. \tag{5}$$

This definition is essentially a local weighted average which converges with mesh refinement to the unique local normal for physically smooth boundaries. For physically nonsmooth corners or intersecting boundaries, special singular bases can be devised (e.g., see [12]).

This approach of requiring strong enforcement of both normal and tangential boundary conditions at dielectric interfaces using (1) contrasts with other usages of this type of basis. In particular, others [5], [13] report the use of scalar bases where all components of E are required to be continuous everywhere, including along dielectric interfaces. Scalar bases used in this way are incapable of resolving physically abrupt changes at such interfaces, and it is not surprising that this practice has produced undesirable results in heterogenous problems.

With this basis, we use the weak form of the Maxwell equations recommended in [10]:

$$\left\langle \frac{1}{j\omega\mu} (\nabla \times E) \times \nabla \phi_i \right\rangle_v + \left\langle \frac{1}{j\omega\mu\epsilon^*} (\nabla \cdot \epsilon^* E) \nabla \phi_i \right\rangle_v + \langle j\omega\epsilon^* E \phi_i \rangle_v = -\oint_S n \times H \phi_i\, ds \tag{6}$$

where the surface integral is performed on the dielectric exterior surface S, $\langle\ \rangle_v$ denotes integration over the enclosed volume, and $n \times H$ is the tangential magnetic field. The surface integral in (6) represents the natural boundary condition and facilitates the coupling between FEM and MoM as formulated in [2]. To complete the discretization, E is expanded as in (1) with strong enforcement of the continuity of $n \times E$ and $n \cdot \epsilon^* E$ at dielectric boundaries as outlined above.

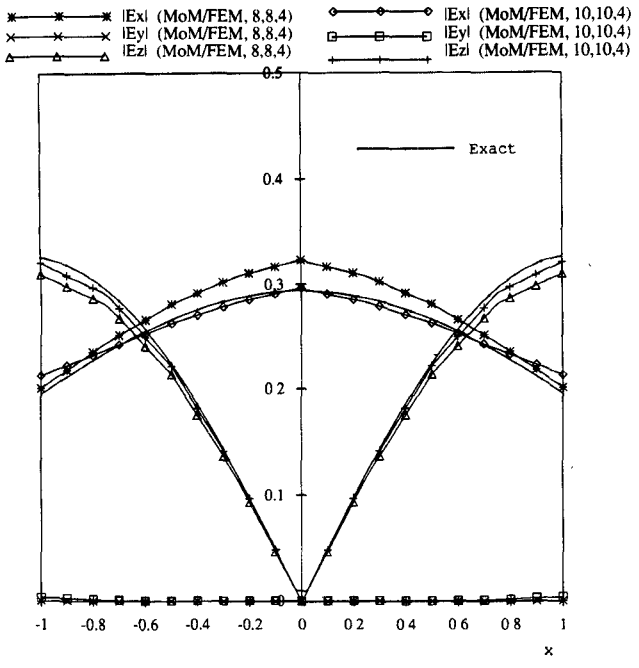

Fig. 1. The magnitude of the electric field inside a homogeneous dielectric sphere along the x axis where $k_0 a = 1/2$, $\epsilon_r = 16$, $\theta^i = \pi$, and $\phi^i = 0$.

III. Numerical Results

In the following, the scattering from a dielectric sphere under the illumination of a plane wave is studied since there exists an analytical (Mie series) solution for comparison. As in [2], the finite element mesh for the sphere consists of both tetrahedra and pentahedra elements and is generated by dividing the radius ($0 \leq r \leq R$) with N_r divisions, the polar angle ($0 \leq \theta \leq \pi$) with N_θ divisions, and the azimuthal angle ($0 \leq \phi \leq 2\pi$) with $2N_\phi$ divisions. (N_θ, N_ϕ, N_r) then denotes the number of divisions used in each model. For example, (8,8,4) indicates that there are eight divisions in θ direction, 16 divisions in ϕ direction, and four divisions in radial direction.

For ease of comparison, we compute the solutions for the same cases as in [2], with identical *geometric* resolution. As a result, there are fewer electromagnetic degrees of freedom in the present calculations. For example, in model (8,8,4) there are 457 nodes which results in 1371 electromagnetic degrees of freedom and a bandwidth of 677 when the scalar basis is used. The corresponding vector basis calculation results in 2856 electromagnetic degrees of freedom with an accompanying bandwidth of 733. Finally, in presenting the results we use the actual bases everywhere, without further interpolation—so the plots are piecewise linear for the scalar

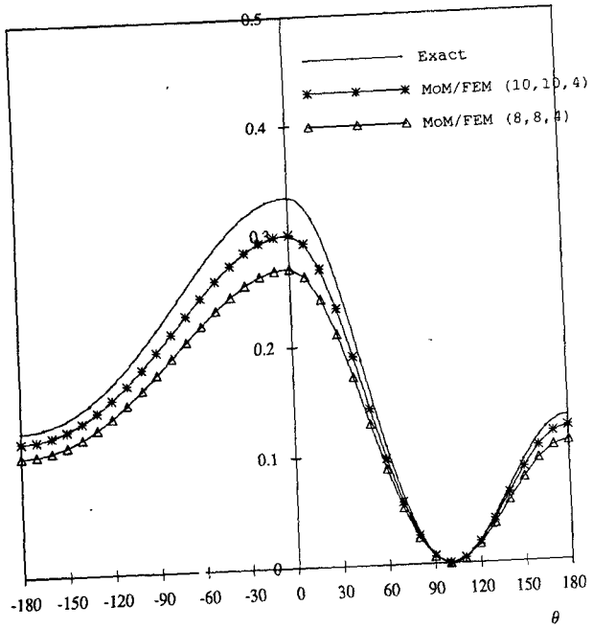

Fig. 2. The radar cross section of the same homogeneous dielectric sphere as in Fig. 1.

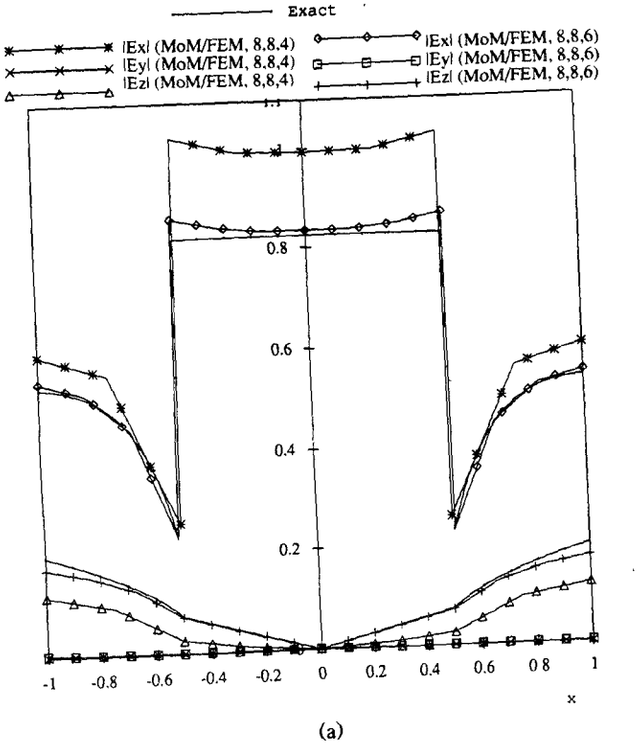

(a)

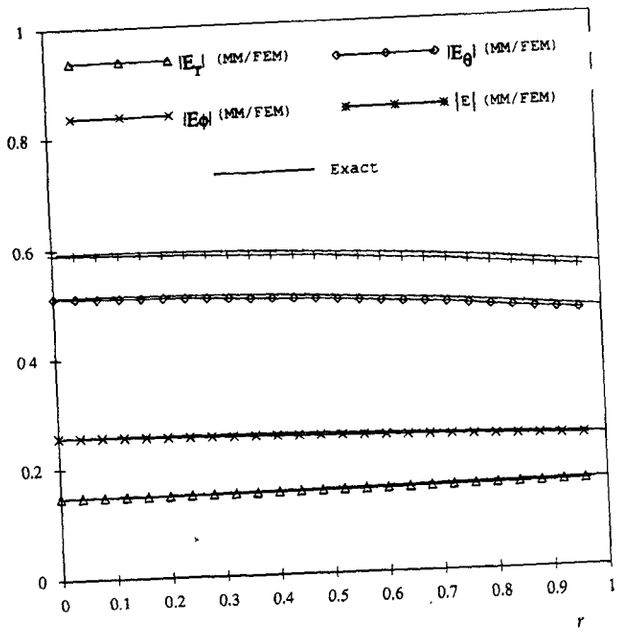

Fig. 3. The magnitude of the electric field inside a homogeneous dielectric sphere along a radial direction ($\theta = \phi = \pi/3$), where $k_0 a = 1/2$, $\epsilon_r = 4$, $\theta^i = \pi$, and $\phi^i = 0$.

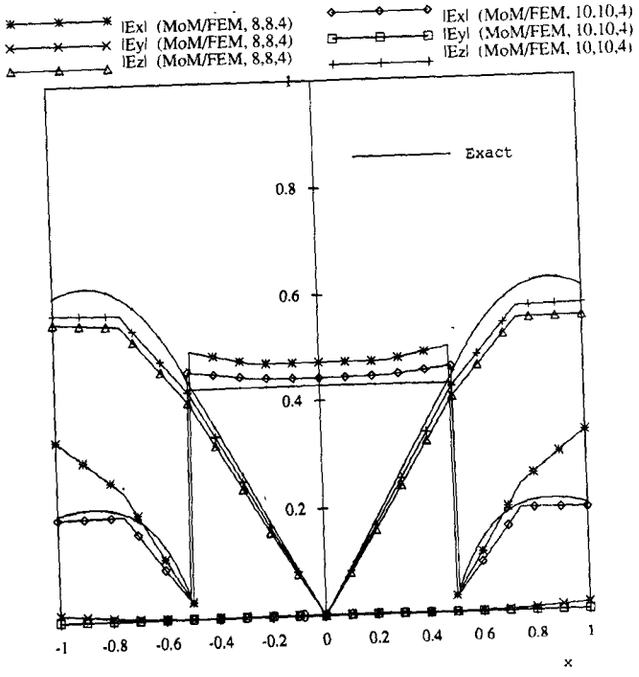

(b)

Fig. 4. The magnitude of the electric field inside a two-layered dielectric sphere along the x axis where $k_0 a_1 = \pi/10$, $\epsilon_{r1} = 1$, $k_0 a_2 = \pi/5$, $\theta^i = \pi$, and $\phi^i = 0$. (a) $\epsilon_{r2} = 4$; (b) $\epsilon_{r2} = 16$.

bases while the vector bases used in [2] have an abrupt, stair-case character.

Fig. 1 shows the magnitude of electric field along the x axis inside a homogeneous sphere under the illumination of an x-directed plane wave, where $k_0 a = 1/2$, $\epsilon_r = 16$, $\phi^i = 0$, $\theta^i = \pi$. The internal field at a given location is computed using (1). Fig. 2 shows the far field of the same sphere as in Fig. 1. Comparing to [2, Fig. (2)], the present piecewise linear solution is superior to the step-wise solution reported in [2]. It is interesting to note that the vector bases used in [2] produce slightly better far field in the forward direction than the scalar bases used here. Fig. 3 shows the magnitude of the electric field along a radial direction ($\theta = \phi = \pi/3$) for a homogeneous sphere, where $k_0 a = 1/2$, $\epsilon_r = 4$, $\phi^i = 0$, $\theta^i = \pi$.

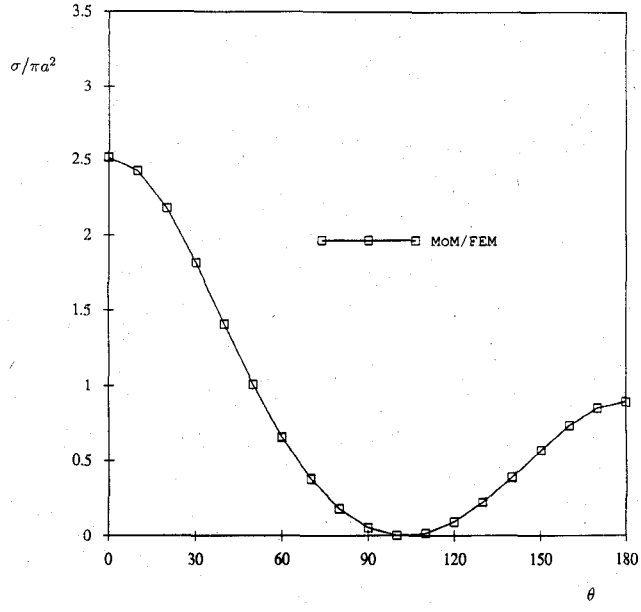

Fig. 5. The radar cross section of a homogeneous dielectric lossy prolate spheroid where $a/b = 2$, $k_o a = \pi/2$, $\epsilon_r = 4$, $\sigma = 0.00417234$, $\theta^i = \pi$, and $\phi^i = 0.0$.

The numerical solutions agree well with the corresponding Mie series (exact) solutions.

Fig. 4 shows the magnitude of the electric field on the x axis for a concentric sphere with inner sphere having radius $a/2$, $\epsilon_{r1} = 1$, and outer sphere having (a) $\epsilon_{r2} = 4.0$ and (b) $\epsilon_{r2} = 16$, where $k_0 a = \pi/5$, $\phi^i = 0$, and $\theta^i = \pi$. On the dielectric interface ($r = a/2$, $\theta = \pi/2$, and $\phi = 0$), E_x is the normal component which should be discontinuous by a factor of 4 and 16, respectively. E_y and E_z are the tangential components which should be continuous. Note that since the interface conditions are enforced strongly, errors at the interface can be amplified by the dielectric contrast. Nonetheless, the solutions shown are quite accurate especially in light of the relatively coarse mesh sizes used. In fact, the solution is dramatically improved by using an (8,8,6) model which represents a modest increase in the number of degrees of freedom. Finally, for completeness we show the radar cross-section of a prolate spheroid in Fig. 5. Good agreement between the scalar and vector basis solutions [2, Fig. 7] is obtained in this case.

IV. Conclusion

The finite element method with an extended weak form and conventional C^0 scalar basis functions is successfully coupled with the method of moments for solving scattering from inhomogeneous 3-D objects. Excellent agreement between the numerical solution and Mie series solution is obtained for both internal and scattered fields. Enforcement of normal conditions on $\boldsymbol{n} \cdot \epsilon^* \boldsymbol{E}$ at dielectric interfaces, in a strong sense, allows relatively coarse discretization of adjacent media, without the complications of wrinkles in previously reported solutions which lacked this important feature. There are no computational drawbacks in terms of run-time or memory requirements relative to the alternative edge elements. To the contrary, the experiments performed to date indicate a modest decrease in these requirements.

References

[1] X. Yuan, D. R. Lynch, and J. W. Strohbehn, "Coupling of finite element and moment methods for electromagnetic scattering from inhomogeneous objects," *IEEE Trans. Anten. Propagat.*, vol. 38, pp. 386–393, Mar. 1990.

[2] X. Yuan, "3-D electromagnetic scattering from inhomogeneous objects by hybrid moment and finite element method," *IEEE Trans. Microwave Theory Tech.*, vol. 38, pp. 1053–1058, Aug. 1990.

[3] M. L. Barton and Z. J. Cendes, "New vector finite elements for three-dimensional magnetic field computation," *J. App. Phys.*, vol. 61, no. 8, pp. 3919–3921, Apr. 1987.

[4] S. H. Wong and Z. J. Cendes, "Numerically stable finite element methods for the Galerkin solution of eddy current problems," *IEEE Trans. Mag.*, vol. 25, no. 4, pp. 3019–3021, July 1989.

[5] A. Bossavit, "Solving Maxwell equations in a closed cavity and the question of spurious modes," *IEEE Trans. Mag.*, vol. 26, no. 2, pp. 702–705, Mar. 1990.

[6] X. Yuan, "On the use of divergenceless vector bases in finite element solution of Maxwell's equations," Dartmouth College Numerical Methods Lab. Rep., 1990.

[7] D. R. Lynch, K. D. Paulsen, and J. W. Strohbehn, "Finite element solution of Maxwell's equations for hyperthermia treatment planning," *J. Comput. Phys.*, vol. 58, pp. 246–269, 1985.

[8] K. D. Paulsen, D. R. Lynch, and J. W. Strohbehn, "Three-dimensional finite, boundary, and hybrid element solutions of the Maxwell equations for lossy dielectric media," *IEEE Trans. Microwave Theory Tech.*, vol. 36, no. 4, pp. 682–693, Apr. 1988.

[9] D. R. Lynch and K. D. Paulsen, "Origin of vector parasites in numerical Maxwell's solutions," *IEEE Trans. Microwave Theory Tech.*, vol. 39, pp. 383–394, Mar. 1991.

[10] K. D. Paulsen and D. R. Lynch, "Elimination of vector parasites in finite element Maxwell solutions," *IEEE Trans. Microwave Theory Tech.*, vol. 39, pp. 395–404, Mar. 1991.

[11] D. R. Lynch and K. D. Paulsen, "Time-domain integration of the Maxwell equations on finite elements," *IEEE Trans. Anten. Propagat.*, vol. 38, pp. 1933–1942, Dec. 1990.

[12] K. D. Paulsen, D. R. Lynch, and J. W. Strohbehn, "Numerical treatment of boundary conditions at points connecting more than two electrically distinct regions," *Commun. App. Numer. Methods*, vol. 3, pp. 53–62, 1987.

[13] G. Mur, "Optimum choice of finite elements for computing three-dimensional electromagnetic fields in inhomogeneous media," *IEEE Trans. Magnet.*, vol. 24, no. 1, pp. 330–333, Jan. 1988.

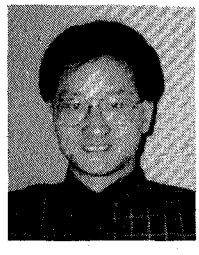

Xingchao Yuan (S'86–M'88) received the B.S. degree in electronic engineering from the Southeast University (previously Nanjing Institute of Technology), Nanjing, China, in 1982, and the M.S. and Ph.D. degrees in electrical engineering from Syracuse University, Syracuse, NY, in 1983 and 1987, respectively.

He served as Research Assistant Professor at Dartmouth College's Thayer School of Engineering, Hanover, NH, from 1987 until 1990. Currently, he is with Ansoft Corp., Pittsburg, PA. His research interests include computational electromagnetics and biomedical applications.

Daniel R. Lynch received the B.S. and M.S. degrees in mechanical engineering from the Massachusetts Institute of Technology, Cambridge, in 1972, and the M.S. and Ph.D. degrees in civil engineering from Princeton University, Princeton, NJ, in 1976 and 1978, respectively.

He has worked as a power engineer and biomedical engineer and is currently Professor at Dartmouth College's Thayer School of Engineering, Hanover, NH, where he has taught since 1978. He directs the Numerical Methods Laboratory at Thayer. His research interests include enviromental engineering and numerical analysis.

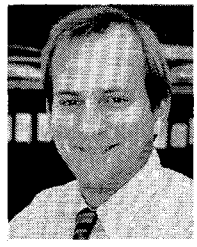

Keith Paulsen (S'85–M'86) received the B.S. degree in biomedical engineering from Duke University, Durham, NC, in 1981, and the M.S. and Ph.D. degrees in engineering from Dartmouth College, Hanover, NH, in 1984 and 1986, respectively.

He served as Assistant Professor in the Department of Electrical and Computer Engineering at the University of Arizona, Tucson, from 1986 to 1988. Currently, he is Assistant Professor at Dartmouth's Thayer School of Engineering, Hanover, NH. His research interests include numerical electromagnetics with application to biomedical problems.